Supporting Information

Discerning the Redox-Dependent Electronic and Interfacial Structures in Electroactive Self-Assembled Monolayers

Raymond A. Wong[†], Yasuyuki Yokota[†,], Mitsuru Wakisaka[‡], Junji Inukai[§] and Yousoo Kim[†,*]*

[†] Surface and Interface Science Laboratory, RIKEN, 2-1 Hirosawa, Wako, Saitama 351-0198, Japan

[‡] Graduate School of Engineering, Toyama Prefectural University, 5180 Kurokawa, Imizu, Toyama 939-0398, Japan

[§] Clean Energy Research Center, University of Yamanashi, 4 Takeda, Kofu, Yamanashi 400-8510, Japan

Email: yyokota@riken.jp, ykim@riken.jp

Non-Ideal Behavior of Fc SAM Cyclic Voltammogram and Relation to HOMO Energy

The non-ideal CV behavior (Figure 1e) as shown by the broad and multiple CV peaks originates from the heterogeneity in intermolecular interactions. Ideal Nernstian behavior is indicated when the CV peak exhibits a FWHM of 90.6 mV which signifies the absence of lateral interactions involving the Fc/Fc^+ termini (i.e. between O-O, R-R and O-R molecules).[1] The deviation from the ideal behavior has been attributed to a variety of reasons including differences in the local packing density (i.e. ordered and disordered domains),[2] isolated and clustered Fc[3] and to buried Fc units.[4] Specifically, the mismatch in dimensions between the diameter of the Fc termini and methylene (CH_2) units of the alkyl chain results in a buildup of strain causing some of the Fc units to become buried and less accessible to the electrolyte[4] leading to possible so-called double layer effects.[5] The presence of multiple peaks is more prominent as the alkyl chain length increases (FcC_nSAu when $n \geq \sim 8$), which is met with an increase in coverage before a saturation in coverage owing to greater favorability in packing energy.[4, 6] The CVs can become closer to exhibiting ideal behavior by reducing the Fc SAM coverage with the co-adsorption of unsubstituted *n*-alkanthiolates.[3]

Regarding the multiple CV peaks and relationship with the HOMO energy, it is important to note that the UPS result neglects a key influencing parameter for the electrochemical response, which is the solvation energy of the electrolyte (solvent and salt).[7] One approach to delineate the relationship between the multiple CV peaks and HOMO energy is the co-adsorption of *n*-alkanethiolates[7] which shows that the single CV peak is accompanied by a single HOMO peak that is comparable in position (binding energy) to the full coverage case[8] thus, suggests the importance of solvation effects from the electrolyte.

Attenuation Length (λ) for Effective Thickness

The determination of effective thickness by XPS (eq. 2) depends on the attenuation length (λ). The attenuation length can be experimental measured from XPS provided the sample is of known thickness, which has been previously done for *n*-alkanethiolates.[9] The estimation of λ can also be performed based on established equations from Seah and Dench[10] or from equations based on so-called TPP-2M methods[11] provided that certain parameters are known (i.e. band-gap energy,

surface coverage, density of overlayer and molecular length etc). A comparison of these λ values for Fc SAMs by Yokota *et al*[12] concluded that λ determined by Bain and Whitesides[9] is comparable to the value determined by equations based on TPP-2M. Therefore, in our work we have used the λ from Bain and Whitesides for the determination of effective thickness for both the Fc and Fc^+ states.

The small change in actual thickness has led to a range of reported values ranging from 0.09-0.3 nm obtained from typical methods such as ellipsometry or surface plasmon resonance (SPR), owing to the need for certain physical parameters to be deduced.[6] For instance, the incident angle used to determine the change in thickness with SPR requires the refractive index (related to dielectric constant) of each layer within the measurement setup to be deduced.[13] Typically, the value of dielectric constant is kept the same for both the Fc and Fc^+ states, which also implies the assumption that there is no ingress of solvent into the SAMs.[6]

Dipole Moment Change of Fc and Fc^+

The work function is related to the change in dipole moment ($\Delta\mu$) can be described with the Helmholtz equation (S1):[14]

$$\Delta\emptyset = \frac{eN\mu}{\varepsilon\varepsilon_0} \qquad \text{(S1)}$$

Where $\Delta\Phi$ as the change in work function, e as elementary charge (1.602×10^{-10} C), N is the dipole density which equates to the surface density of Fc SAM, while ε and ε_o are the relative dielectric constant for n-alkanethiolates (3.4) and vacuum permittivity (8.55×10^{-12} F m^{-1}), respectively. Relative to the Au metal surface, for the Fc state, we obtain $\Delta\mu = 7.6 \times 10^{-30}$ C m or 2.28 D (Debye, D = 3.336×10^{-30} C m). In the Fc^+ state we obtain $\Delta\mu = 1.09 \times 10^{-30}$ C m or 0.33 D. The resulting change in dipole moment of the two states is therefore, -6.52×10^{-30} C m or -1.95 D (negative denotes the change), which would be comparable in magnitude to partially fluorinated akanethiolate SAMs.[15]

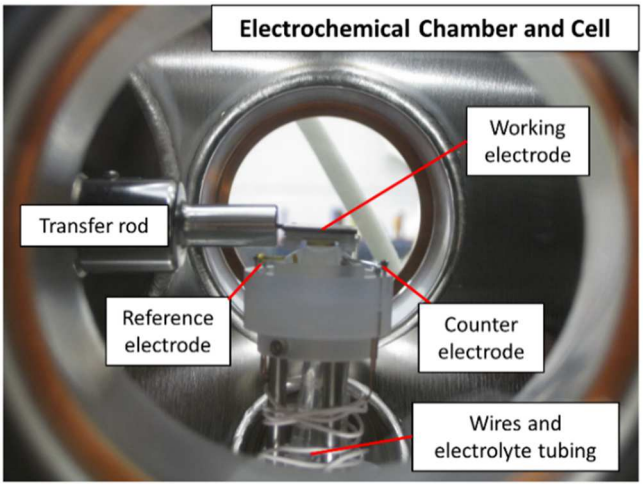

Figure S1. Digital photograph showing the interior of the electrochemical (EC) chamber. The EC cell is in the typical position for EC measurements. The hanging meniscus is visible in the photograph.

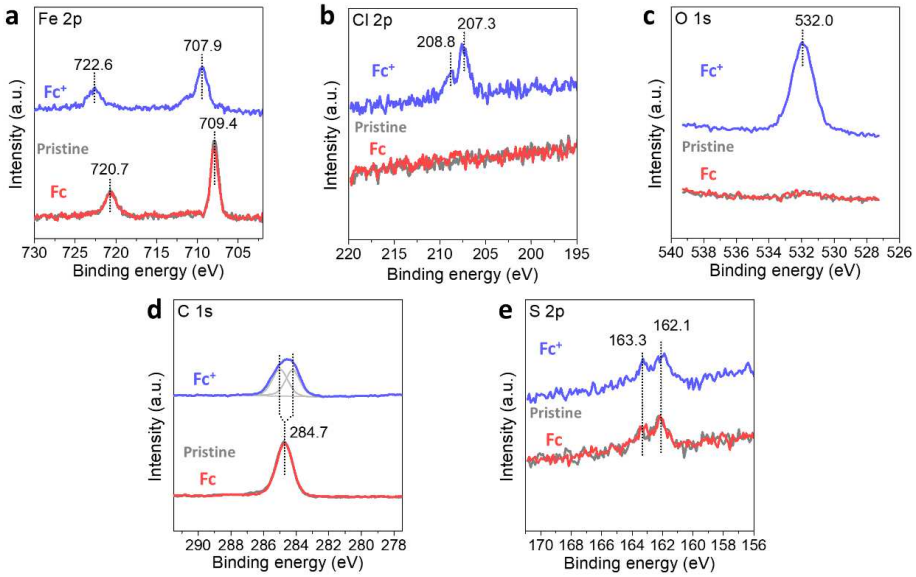

Figure S2. XPS of pristine Fc SAMs after polarization at 0.5 and 0.1 V in 0.1 M $NaClO_4$, corresponding to the oxidized Fc^+ and neutral Fc states, respectively. The pristine and Fc spectra have been overlaid together. (a) Fe 2p, (b) Cl 2p, (c) O 1s, (d) C 1s and (e) S 2p spectra. The data correspond to Figure 2 in the main text. The overlaid Au 4f spectra can be found in the main text.

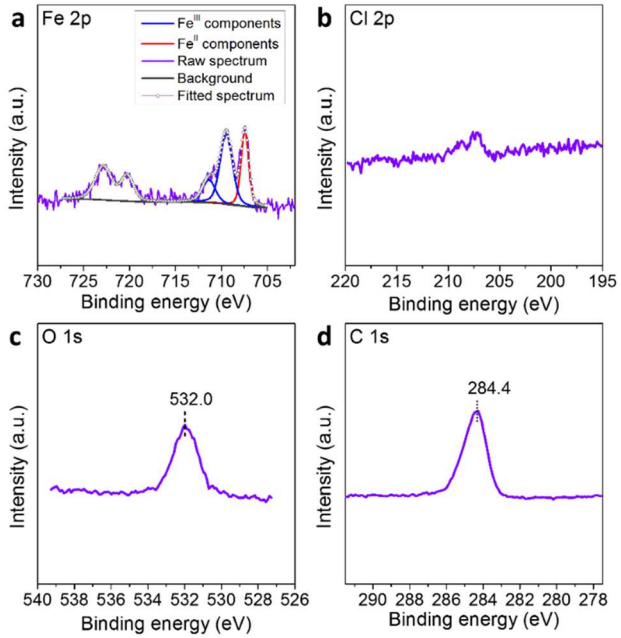

Figure S3. XPS following anodic polarization at 0.37 V (corresponding to the second oxidation peak) in 0.1 M $NaClO_4$. The presence of mixed valence states of Fc/Fc^+ is observed. (a) Fitted Fe 2p spectrum with the Fe $2p_{1/2}$ fitting omitted for clarity (b) Cl 2p, (c) O 1s, and (d) C 1s spectra. The Fe^{III}:Fe^{II} area ratio is 1:0.5, which equates to ~67% of the Fc as being oxidized.

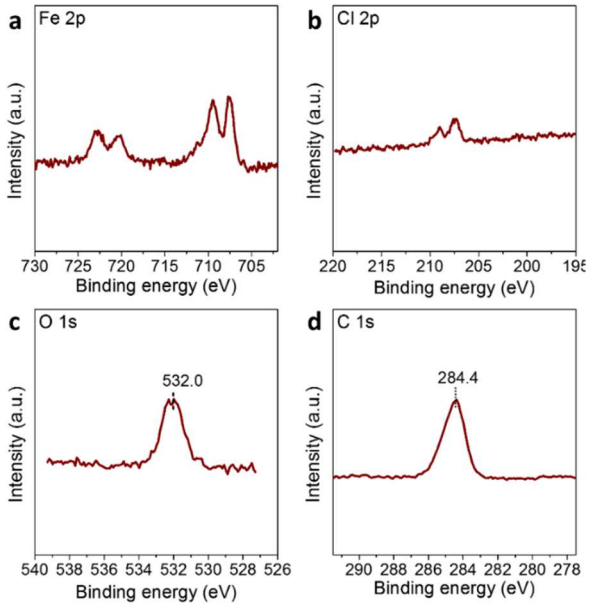

Figure S4. XPS following cathodic polarization at 0.1 V in 0.1 M $HClO_4$. (a) Fe 2p, (b) Cl 2p, (c) O 1s, and (d) C 1s spectra. Despite polarization at a cathodic potential, there is the presence of mixed Fc/Fc^+ states.

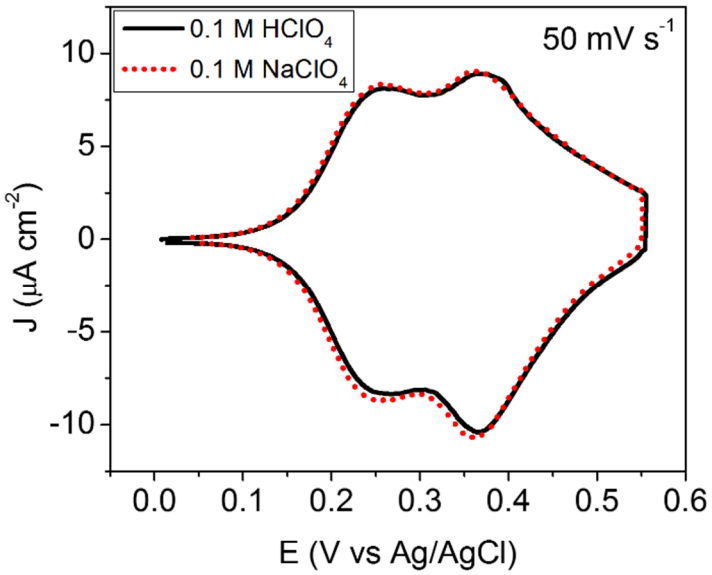

Figure S5. Cyclic voltammograms in 0.1 M $HClO_4$ and $NaClO_4$ performed at the scan rate of 50 mV s^{-1}. The formal potentials and EC response in the two electrolytes are have been reported to be virtually identical.[16]

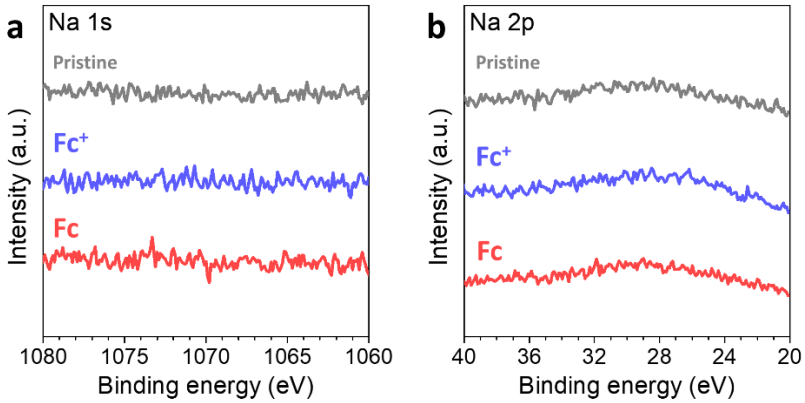

Figure S6. XPS of pristine Fc SAM electrode and following polarization at 0.5 and 0.1 V in 0.1 M $NaClO_4$ to yield Fc^+ and Fc, respectively. (a) Na 1s, and (b) Na 2p spectra. In all, the XPS results show that there is no incorporation of Na species.

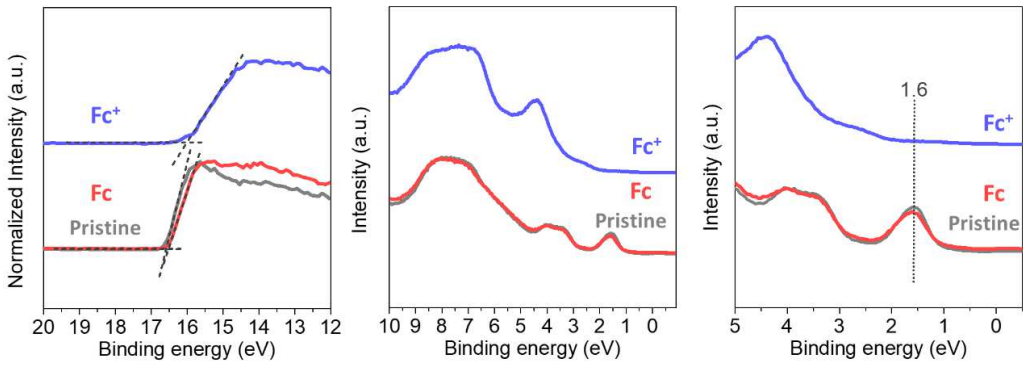

Figure S7. UPS spectra of the pristine Fc SAMs and after polarization at 0.5 and 0.1 V corresponding to oxidized Fc^+ and neutral Fc states, respectively. The pristine and Fc spectra are overlaid together and are identical to Figure 5. (left panel) Secondary electron cutoff region. (middle panel) HOMO emission region. (right panel) Enlarged HOMO emission region near the Fermi level. The work function and HOMO energy of pristine and Fc are within 0.1 eV of each other.

REFERENCES

1. Vogel, Y. B.; Zhang, L.; Darwish, N.; Gonçales, V. R.; Le Brun, A.; Gooding, J. J.; Molina, A.; Wallace, G. G.; Coote, M. L.; Gonzalez, J., Reproducible flaws unveil electrostatic aspects of semiconductor electrochemistry. *Nat. Commun.* **2017,** *8*, 2066.
2. Uosaki, K.; Sato, Y.; Kita, H., Electrochemical characteristics of a gold electrode modified with a self-assembled monolayer of ferrocenylalkanethiols. *Langmuir* **1991,** *7*, 1510-1514.
3. Lee, L. Y. S.; Sutherland, T. C.; Rucareanu, S.; Lennox, R. B., Ferrocenylalkylthiolates as a probe of heterogeneity in binary self-assembled monolayers on gold. *Langmuir* **2006,** *22*, 4438-4444.
4. Nerngchamnong, N.; Thompson, D.; Cao, L.; Yuan, L.; Jiang, L.; Roemer, M.; Nijhuis, C. A., Nonideal Electrochemical Behavior of Ferrocenyl–Alkanethiolate SAMs Maps the Microenvironment of the Redox Unit. *J. Phys. Chem. C* **2015,** *119*, 21978-21991.
5. Creager, S. E.; Rowe, G. K., Solvent and double-layer effects on redox reactions in self-assembled monolayers of ferrocenyl—alkanethiolates on gold. *J. Electroanal. Chem.* **1997,** *420*, 291-299.
6. Feng, Y.; Dionne, E. R.; Toader, V.; Beaudoin, G.; Badia, A., Odd–Even Effects in Electroactive Self-Assembled Monolayers Investigated by Electrochemical Surface Plasmon Resonance and Impedance Spectroscopy. *J. Phys. Chem. C* **2017,** *121*, 24626-24640.
7. Yokota, Y.; Mino, Y.; Kanai, Y.; Utsunomiya, T.; Imanishi, A.; Wolak, M. A.; Schlaf, R.; Fukui, K., Comparative studies of photoelectron spectroscopy and voltammetry of ferrocene-

terminated self-assembled monolayers possessing different electron-donating abilities. *J. Phys. Chem. C* **2014,** *118*, 10936-10943.
8. Mendez De Leo, L. P.; de la Llave, E.; Scherlis, D.; Williams, F. J., Molecular and electronic structure of electroactive self-assembled monolayers. *J. Chem. Phys* **2013,** *138*, 114707.
9. Bain, C. D.; Whitesides, G. M., Attenuation lengths of photoelectrons in hydrocarbon films. *J. Phys. Chem.* **1989,** *93*, 1670-1673.
10. Seah, M. P.; Dench, W., Quantitative electron spectroscopy of surfaces: A standard data base for electron inelastic mean free paths in solids. *Surf. Interface Anal* **1979,** *1*, 2-11.
11. Kondo, T.; Yanagida, M.; Shimazu, K.; Uosaki, K., Determination of thickness of a self-assembled monolayer of dodecanethiol on Au (111) by angle-resolved X-ray photoelectron spectroscopy. *Langmuir* **1998,** *14*, 5656-5658.
12. Yokota, Y.; Mino, Y.; Kanai, Y.; Utsunomiya, T.; Imanishi, A.; Fukui, K., Electronic-State Changes of Ferrocene-Terminated Self-Assembled Monolayers Induced by Molecularly Thin Ionic Liquid Layers: A Combined Atomic Force Microscopy, X-ray Photoelectron Spectroscopy, and Ultraviolet Photoelectron Spectroscopy Study. *J. Phys. Chem. C* **2015,** *119*, 18467-18480.
13. Yao, X.; Wang, J.; Zhou, F.; Wang, J.; Tao, N., Quantification of redox-induced thickness changes of 11-ferrocenylundecanethiol self-assembled monolayers by electrochemical surface plasmon resonance. *J. Phys. Chem. B* **2004,** *108*, 7206-7212.
14. Yuan, L.; Thompson, D.; Cao, L.; Nerngchangnong, N.; Nijhuis, C. A., One carbon matters: The origin and reversal of odd–even effects in molecular diodes with self-assembled monolayers of ferrocenyl-alkanethiolates. *J. Phys. Chem. C* **2015,** *119*, 17910-17919.
15. Alloway, D. M.; Hofmann, M.; Smith, D. L.; Gruhn, N. E.; Graham, A. L.; Colorado Jr, R.; Wysocki, V. H.; Lee, T. R.; Lee, P. A.; Armstrong, N. R., Interface Dipoles Arising from Self-Assembled Monolayers on Gold: UV− Photoemission Studies of Alkanethiols and Partially Fluorinated Alkanethiols. *J. Phys. Chem. B* **2003,** *107*, 11690-11699.
16. Redepenning, J.; Flood, J. M., Influence of Electrolyte Activity on Formal Potentials Measured for Ferrocenylhexanethiol Monolayers on Gold: Indistinguishable Responses in Aqueous Solutions of $HClO_4$ and $NaClO_4$. *Langmuir* **1996,** *12*, 508-512.